


 Cite this: *RSC Adv.*, 2020, **10**, 5785

Fluorescent characteristics of dissolved organic matter released from biochar and paddy soil incorporated with biochar[†]

 Jiakai Gao,^{ab} Zhaoyong Shi,^a Haiming Wu^b and Jialong Lv^{*bc}

Dissolved organic matter (DOM) plays a critical part in many processes of the ecological environment due to its mobility and reactivity in the soil and water interface. In the presented study, excitation-emission matrices (EEM) coupled with parallel factor analyses (PARAFAC) and UV-visible spectroscopy were introduced to investigate the variation of DOM derived from wheat straw biochar produced at different pyrolysis temperatures (300 °C, 500 °C and 700 °C), qualitatively and quantitatively. The dissolved organic matter (DOM) content of 700 °C biochar achieved a maximum of 1.45 g kg⁻¹, while a minimum of 0.61 g kg⁻¹ was found at 500 °C. Components consisting of protein and tryptophan-like, UVA humic acid-like and UVC humic acid-like substances were extracted from the fluorescence data using PARAFAC. The abundance of fluorescent components predicted that DOM was mainly composed of more aromatic humic materials and litter amino acids with the increase in the pyrolysis temperature. Additionally, a column experiment simulating a paddy field was conducted to evaluate the feasible application of biochar produced at different temperatures, and the results showed that biochar addition enhanced the aromaticity and accelerated the decomposition of DOM released from flooded paddy soil. However, the indices SUVA₂₅₄ and SUVA₂₆₀ showed increasing tendencies in the soil profile, which may be ascribed to the downward transport of water-soluble DOM during the period of leaching. Briefly, the findings obtained, reinforced by statistical analysis could provide some valuable and distinct optical information of DOM derived from biochar and offer technical guidance when incorporating biochar into paddy soil in agricultural production.

 Received 7th December 2019
 Accepted 29th January 2020

DOI: 10.1039/c9ra10279e

rsc.li/rsc-advances

1. Introduction

To relieve pressure on the agricultural environment by chemical fertilization, crop residues and their derivatives are advocated to regulate the migration and transformation of soil nutrients such as carbon, nitrogen and phosphorus in paddy fields. As a renewable energy resource, wheat straw offers an immense potential function in producing biogas, biofuel and biochar in

a green-sustainable development trend, and of the utilization modes mentioned above, biochar has received a favourable reception for its beneficial applications in recent years.^{1,2}

Biochar, a carbon-rich organic substance produced by crop residues or biomass under limited-oxygen conditions, contains abundant aromatic compounds composed of stable fractions and is resistant to degradation by microorganisms.³⁻⁵ In recent years, there have been increasing studies investigating the soil nutrient cycle, crop yield and quality, and greenhouse gas (GHG) emissions under biochar amendments, which suggests that biochar application could improve soil quality and reduce GHG emissions by regulating physicochemical properties (such as soil porosity, organic carbon, and pH), the structure of the microbial community and microbial activities.⁶⁻⁸ Previous studies mainly focused on the variations of GHG emission, changes in the soil carbon fraction and crop yield after biochar application through a field experiment and had little consideration of the DOM in the leached water from topsoil. Many former researchers revealed that biochar amendments could increase the soil DOM content and alter its composition, which may play a vital role in the fate and transport of soil contaminants, including heavy metals and organic pollutants.⁹⁻¹² Therefore, there has been a push to further our understanding of the soluble organic fraction of biochar-

^aCollege of Agriculture, Henan University of Science and Technology, Luoyang, 471023, PR China

^bCollege of Natural Resources and Environment, Northwest A&F University, Yangling, Shaanxi, 712100, PR China. E-mail: ljl11@nwsuaf.edu.cn

^cKey Laboratory of Plant Nutrition and the Agri-environment in Northwest China, Ministry of Agriculture, Yangling, Shaanxi, 712100, PR China

[†] Electronic supplementary information (ESI) available: Fig. S1 diagram of the soil column experimental design (column height: 50 cm, inner diameter: 10 cm). Wheat straw biochar of different pyrolysis conditions combined with fertilizer levels was mixed with the 0–10 cm soil layer (i.e., CK: control treatment without biochar and fertilizer; CF: conventional fertilizer applied; RF: fertilizer reduced 20% compared with CF; FBC300: 300 °C biochar combined with RF; FBC500: 500 °C biochar combined with RF; FBC700: 700 °C biochar combined with RF). Silica sands were placed at the bottom to maintain column aeration, and unwoven straw was twined at the inward sampling mouth to guard against blocking. See DOI: 10.1039/c9ra10279e



derived DOM and soil DOM from biochar amendments.^{5,13} Additionally, the DOM contents of biochar were determined by the pyrolysis conditions, including pyrolysis temperature, carbonization time and oxygen supply, and of the parameters mentioned above, the pyrolysis temperature has a significant effect on the physicochemical properties (such C%, N%, C/N, cation exchange capacity, and specific area) and then influences the DOM characteristics indirectly.^{14,15}

The optical properties of DOM, especially its UV-visible absorbance and fluorescence, are typically examined for the purpose of DOM composition.¹⁶ Researchers also suggested the DOM aromaticity increased with the increasing pyrolysis temperature of biochar through the UV-visible tool.¹⁷ In addition, excitation-emission matrix (EEM) fluorescence combined with a parallel factor analysis (PARAFAC) was also employed to identify the DOM components based on the excitation and emission (Ex/Em) maxima.^{18–21} Overwhelmingly, PARAFAC modelling could collect several independent fluorophore groups that expressed similar fluorescence features from their lapped mixture of the EEM spectra and offer specific information of samples.²² Hence, EEM-PARAFAC was accepted as a powerful and sensitive technique in characterizing the DOM composition in freshwater, soil and organic materials.^{10,23} Presently, studies that focus on the characterization of DOM from waterlogged paddy soil after the soil column leaching are limited, and further investigation is warranted.

In this study, we hypothesis application of biochar obtained at three temperatures varied soil DOM fraction of fluorescent materials after a soil column simulate trial, which was significant to understanding the DOM dynamics in the process of leaching. Herein, the main objects of this study were to (1) investigate the dynamics of DOC concentrations in leaching solutions; (2) characterize the composition and structure of soil DOM by means of spectroscopic techniques; and (3) gain the fluorescence components using PARAFAC modelling and analyse the variations of relevant optical indices. To our knowledge, this is the first work to explore the DOM spectrum features in vertical paddy soil (0–40 cm) incorporated with or without fertilizer/biochar after leaching.

2. Materials and methods

2.1 Preparation of soil and biochar in this study

Soil in this study was collected on 25 September 2017 (after the rice harvest) from our test site, located in Xinji County ($33^{\circ}0'16''N$, $108^{\circ}48'44''E$) Hanzhong City. Four soil layers (0–10, 10–20, 20–30, and 30–40 cm) in this study were collected from the local farmland, dominated by a wheat and rice system. Measurements of basic physicochemical properties of tested soil were conducted according to standard analysis methods. Wheat straw was used for biochar production with the following procedure. After air-drying and crushing, the crushed wheat straw was filled into crucibles sealed with lids to prevent oxygen from entering and then pyrolyzed in a muffle furnace, heating at a rate of $10\text{ }^{\circ}\text{C min}^{-1}$, and holding at 300, 500, and 700 $^{\circ}\text{C}$ for 2 h.²⁵ The biochars produced with low (300 $^{\circ}\text{C}$), medium (500 $^{\circ}\text{C}$), and high (700 $^{\circ}\text{C}$) temperatures were denoted by BC300,

BC500, and BC700, respectively. The details of soil and biochar used in the presented study are described in Table S1.[†]

2.1.2 Experimental setup. To simulate wheat straw biochar amendment in flooded paddy soil, a series of soil column experiments were conducted in Yangling District, Shaanxi Province, China ($34^{\circ}15'N$, $108^{\circ}34'E$). Approximately 1 kg of air-dried soil was placed in a soil column every 10 cm in height (Fig. S1†), and the 0–10 cm layer was mixed with 3% of the biochars from different pyrolysis temperatures at a reduced fertilizer level (*i.e.*, CK: control treatment without biochar and fertilizer; CF: conventional fertilizer applied; RF: reduced 20% fertilizer compared with CF; FBC300: 300 $^{\circ}\text{C}$ biochar combined with RF; FBC500: 500 $^{\circ}\text{C}$ biochar combined with RF; FBC700: 700 $^{\circ}\text{C}$ biochar combined with RF).²⁶ Then, 1350 mL of deionized water was added to saturate the dried soil in the column. Deionized water was added to keep the surface water volume at 300 mL in the process of the whole experiment. At the end of leaching, soils in different layer from column were collected, air dried and sieved for further determination.

2.2 Analytical methods

2.2.1 Preparation of soil and biochar DOM extracts. The solutions for fluorescence and the UV-Vis spectrum analysis to determine the soil DOM chemical structure were extracted by deionized water with a 1 : 6 w/v ratio of water and sieved soil (through 100 mesh sieves). The mixture was then centrifuged (4000 rpm) at room temperature for 20 min after shaking on a mechanical platform shaker at 180 rpm in the dark for 24 h. However, biochar (1 g) was taken in plastic centrifuge tubes and mixed with 20 mL of deionized water. Then, the tubes were placed horizontally on a mechanical platform shaker (180 rpm) in the dark for 2 h. The suspensions were centrifuged at 10 000 rpm for 10 min. Finally, the obtained supernatants were filtered through 0.45 mm microfiber filters (Millipore) and maintained in the dark at 4 $^{\circ}\text{C}$ for further DOM analysis.

2.2.2 UV-vis and fluorescence spectrum analysis. The quantities of samples' DOM were represented by DOC concentrations, which were measured with a total organic carbon (TOC) analyser (Shimadzu Inc., TOC-VCHP, Japan). A UV-Vis spectrophotometer (UV Probe-1780, Shimadzu, Japan) was utilized to determine the absorbance values of water-extractable DOM, and deionized water was used to prepare a baseline at wavelengths of 400–250 nm.

For the fluorescence intensity measurement, a three-dimensional excitation-emission matrix (3D-EEM) was studied by employing a fluorescence spectrophotometer (F97 Pro, Lengguang Tech., China), scanning at excitation wavelengths ranging from 200 to 500 nm and emission wavelengths from 250 to 550 nm, with an increment of 5 nm. The scanning speed was set at 6000 nm min^{-1} . A blank solution (deionized water) was taken into consideration to obtain emission spectra solely from DOM samples by subtracting the blank signals from the measured fluorescence. In the case of the UV absorbance coefficient at 254 nm over 0.05, the DOM solution samples should be diluted prior to fluorescence determination to prevent inner-filter collection.²⁷



PARAFAC modelling was operated through MATLAB 7.0 (Mathworks, Natick, MA, USA) coupled with the DOM Fluor Toolbox following the recommendation of Stedmon and Bro (2008).¹⁸ In our study, 9 biochars and 72 soil DOM samples were prepared to obtain EEM spectra, which were utilized for PARAFAC modelling calculations.

To evaluate the environmentally relevant UV parameters in the present study, data were used selectively to calculate SUVA₂₅₄ (specific UV absorbance at wavelength 254 nm) and *S_R* (slope ratio). In addition, DOM characteristics were also investigated by the fluorescent indices, which have been shown to relate to DOM structure: (i) the humification index (HIX), an indication of the humification degree (Zsolnay, 2001);²⁸ (ii) the fluorescence index (FI), which is used to distinguish DOM sources from terrestrial or microbial sources (McKnight *et al.*, 2001);²⁹ (iii) the biological index (BIX), which reflects the ratio of albuminoid and biological components;³⁰ and (iv) the ratio of two fluorescing components ($\beta : \alpha$), where β represents recent labile OM (often microbially produced or autochthonous) and α represents recalcitrant OM (allochthonous).³⁰

2.3 Statistical analysis

The raw data were addressed using Excel 2010 (Microsoft Excel 2010, O'Reilly, Microsoft USA). All figures in this work were drawn with Origin 9.0 (Origin 2015, USA). Data were processed statistically with analysis of variance (ANOVA) and Duncan's multiple range tests for significant differences between treatments at $p < 0.05$. All data analysis was conducted using the SPSS 20.0 (SPSS Inc., Chicago, USA) software package.

3. Results and discussion

3.1 Quantity of DOM derived from biochar and soil

Generally, the soluble organic C fraction in the DOM pool can be represented by the DOC concentration.^{11,31} The content of DOC derived from the biochar produced at different pyrolysis temperatures (300, 500 and 700 °C) is shown in Table S1.† DOC extracted from biochar at the three temperatures varied significantly, and the mean DOC concentration of biochar at 300 °C (1.14 g kg⁻¹) was higher than that observed at 500 °C (0.61 g kg⁻¹) ($p < 0.05$), which suggested the notable effect of the pyrolysis temperature on DOM release from wheat straw biochar. These findings contrast with previous studies that found that biochar produced at low temperature had a higher DOC content compared to biochar obtained at higher temperatures.^{32,33} However, with the increase in the pyrolysis temperature, the DOC content significantly increased at 700 °C (1.45 g kg⁻¹) ($p < 0.05$) compared to the biochar produced at low temperatures. Meanwhile, higher temperature may lead to a secondary reaction during the pyrolysis producer, which resulting in a lower DOC content.³² Hence, in the present study, wheat straw biochar produced at 700 °C has a potential higher release of DOM and can be recommended as a favourable material in possible applications for wastewater treatment, soil remediation or other environmental fields.

To evaluate the effect of biochar amendments on the soil DOM content, the water-extractable DOC contents of different treatments (*i.e.*, CK: control treatment without biochar and fertilizer; CF: conventional fertilizer applied; RF: reduced 20% fertilizer compared with CF; FBC300: 300 °C biochar combined with RF; FBC500: 500 °C biochar combined with RF; FBC700: 700 °C biochar combined with RF) in the soil profile (0–40 cm) was also determined (Fig. 1). Overall, the mean DOC contents in the soil profile were in the range of 0.064–0.088 g kg⁻¹, while the mean DOC content of the third layer (20–30 cm) was the highest (0.088 g kg⁻¹) ($p < 0.05$), which may be attributed to the accumulation of DOC during the process of leaching. DOC concentrations in soil with amendments of biochar produced at the three temperatures were significantly higher than those of CK, CF and RF ($p < 0.05$), which indicated that biochar supplements could increase the soil DOC content compared to the control treatment without biochar. Similar studies have shown that soil DOC significantly increased from 84 to 144 mg kg⁻¹ markedly with biochar amendment.⁵ In addition, the increasing of soil DOM could also be attributed to the high pH of biochar, which produce some soil minerals coupled with negative charge, resulting in the desorption of positive DOC (Tang *et al.*, 2016).¹¹ Moreover, human activities in agricultural production, including fertilization, irrigation, and the addition of organic materials such as crop residues, feed stocks and biochar, could induce the strong variations in soil DOC,⁶ which was found in the treatments with biochar combined with fertilizer in this study. Wardle *et al.* (2008) also revealed that biochar application offered a possible increase in soil organic carbon lability,³⁴ which could enhance the soil microbial biomass and activity effectively. However, in the other three soil

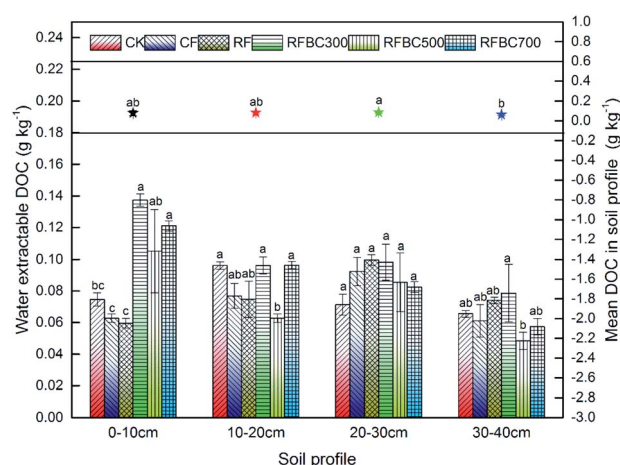


Fig. 1 The content of DOM (represented by DOC concentration) from soils sampled after the leaching test. Different coloured bars represent different treatments (treated in the 0–10 cm layer) (*i.e.*, CK: control treatment without biochar and fertilizer; CF: conventional fertilizer applied; RF: fertilizer reduced 20% compared with CF; FBC300: 300 °C biochar combined with RF; FBC500: 500 °C biochar combined with RF; FBC700: 700 °C biochar combined with RF). All values are given as the mean \pm SD from three replicates. Different letters indicate statistical differences between different pyrolysis temperature treatments ($p < 0.05$).



profiles, there were no significant differences among all treatments, as well as the biochar addition treatments.

3.2 EEM-PARAFAC components and its distribution in biochar

In this study, the three fluorescent components (labelled C1, C2 and C3, respectively) of DOM released from biochars produced at different pyrolysis temperatures were identified by fluorescence EEM and PARAFAC analyses. As shown in Fig. 2, EEM-PARAFAC C1, C2 and C3 and the corresponding spectral loadings were presented. In addition, the characteristics of the three identified components were summarized in Table 1 in detail. The results in this study showed that the identified components comprised one protein- and tryptophan-like substance (C1) and two humic acid-like substances [C2 (UVA humic acid-like), C3 (UVC humic acid-like)]. The C1 component was characterized by peaks at 245 (265) nm excitation and 380 nm emission wavelengths, and C1 was defined as a protein- and tryptophan-like substance, which indicated intact proteins or less degraded peptide material.^{22,27,35} The C2 component was characterized by peaks at 220 nm excitation and 410 (420) nm emission wavelengths, and the component was described as a UVA humic acid-like compound with low-molecular-weight material, which was common in wetlands and agricultural environments.^{23,36,37} The C3 component was characterized by peaks at 260 (280) nm excitation and 440 (480) nm emission wavelengths, and it was regarded as a UVC humic acid-like compound with high molecular weight and aromatic humic,

which agreed with the humic acid-like materials identified by EEM-PARAFAC.^{10,36-38} The probable sources of C1 and C2 were considered as autochthonous, terrestrial or soil organic matter or microbial processes, while C3 was deemed to be from terrestrial or soil organic matter.^{16,39} Additionally, the relative abundances of PARAFAC C1, C2 and C3 were also analysed in Fig. 2D. The relative abundances of the three fluorescent components (C1–C3) of DOM released from biochar at 300 °C accounted for 38.39%, 42.19% and 19.41%, respectively, which indicated a major presence of UVA humic acid-like substance. Similarly, C2 was the main contributor of DOM derived from 500 °C biochar, which accounted for 47.92% of the three PARAFAC components. However, the DOM composition released from biochar produced at 700 °C was dominated by UVC humic acid-like material (47.68%). It also should be noted that the proportions of protein- and tryptophan-like substances (C1) were significantly decreased with the increase in pyrolysis temperature (300 °C: 38.39%, 500 °C: 25.05%, 700 °C: 10.69%), which poorly predicted the amino acids released during the process of the temperature increase. However, the percentages of UVC humic acid-like substances (C3) were raised notably with the increasing pyrolysis temperature (300 °C: 19.41%, 500 °C: 27.03%, 700 °C: 47.68%). These results suggested more high-molecular-weight and aromatic humic materials generated when the pyrolysis temperature increased from 300 °C to 700 °C. The above results are in agreement with those conclusions in previous studies. The EEM-PARAFAC technique was used to quantify the DOM

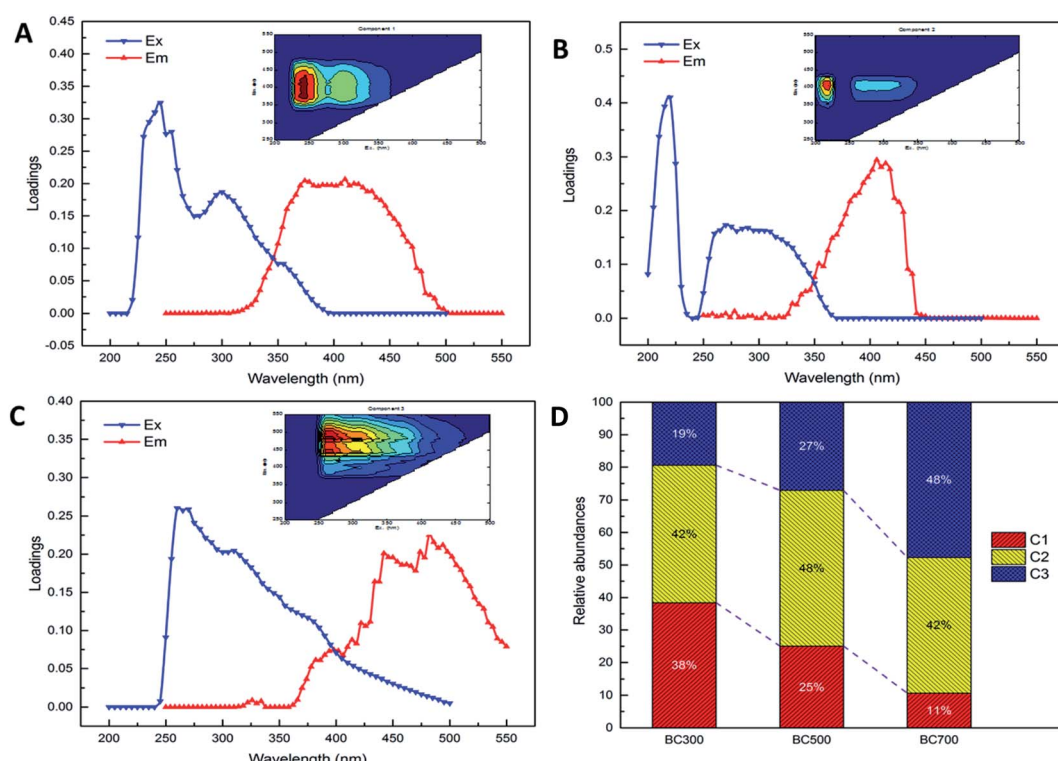


Fig. 2 Representative EEM contours, fluorescence spectral loadings and the distributions of the three components identified by EEM-PARAFAC analysis. Ex: excitation wavelength; Em: emission wavelength. (A) component 1, (B) component 2, (C) component 3, (D) relative distributions of C1, C2 and C3.



Table 1 Characteristics of the three components identified via EEM-PARAFAC analysis. Ex: excitation wavelength; Em: emission wavelength^a

Components	EEM locations	Fluorescent substance	Descriptions and assignment	Probable source ^{16,39}	References
C1	Ex = 245 (265) nm, Em = 380 nm	Protein- and tryptophan-like	Amino acids, free or bound in protein, may indicate intact proteins or less degraded peptide material	A, T, M	22, 27 and 35
C2	Ex = 220 nm, Em = 410 (420) nm	UVA humic acid-like	Low molecular weight, common in wetlands and agricultural environments	A, T, M	23, 36 and 48
C3	Ex = 260 (280) nm, Em = 440 (480) nm	UVC humic acid-like	High molecular weight and aromatic humic, highest in wetlands and forested environments	T	36, 38, 47 and 48

^a A, autochthonous; T, terrestrial or soil organic matter; M, microbial process.

composition of biochar and showed that biochar-amended DOM released mainly humic acid fractions during a field trial.^{24,40} Hydrophobic acid, humic acid or marine humic acid-like substances were also observed from DOM derived from biochar produced at different temperatures.^{10,11}

To better understand the variability of DOM derived from biochar produced at different pyrolysis temperatures (300, 500 and 700 °C), the relative abundances of DOM components were evaluated in terms of the fluorescence intensity (Fig. 3). Overall, the mean fluorescence intensities of PARAFAC components in biochar produced at 300 °C (472.41) were significantly higher than those of biochar produced at 500 °C (19.45) and 700 °C (1.45). Specifically, the fluorescence intensities of C1 and C2 of DOM released from 300 °C biochar were markedly higher than that of C3, which showed an abundance of aromatic humic materials. Nevertheless, the fluorescence intensity of C2 of DOM released from biochar produced at 700 °C was the dominant compound compared to C1 and C3. Furthermore, the

fluorescence intensities of C1, C2 and C3 were found to have little difference in the DOM released from 500 °C biochar.

To summarize, the results obtained in this study indicated that the pyrolysis temperature significantly regulated the distribution of different components of DOM released from biochar. Several studies also suggested that the DOM content and composition were greatly influenced by the biochar feedstocks, pyrolysis conditions and extractable producer.^{41,42} Lin *et al.* reported that the lower DOM was obtained in the high temperature biochar, which consisted of more low-molecular-weight acids.³² Mukherjee *et al.* also noted that the quantity of DOM derived from biochar was closely related to the contents of acid functional groups and volatile matter.³³

3.3 Optical indices of DOM derived from biochar and soil

To elucidate the chemical characteristics of DOM released from the biochar produced at different pyrolysis temperatures, the

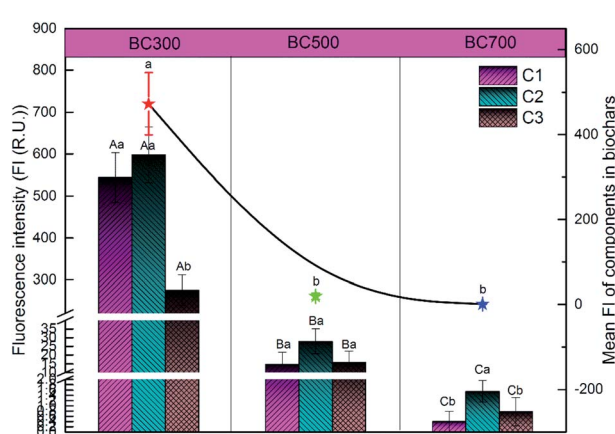


Fig. 3 Fluorescence intensity (FI) of the three components (C1, C2 and C3) and mean FI of components in biochar produced at different pyrolysis temperatures (300, 500 and 700 °C). All values are given as the mean \pm SD from three replicates. Different letters indicate statistical differences between different pyrolysis temperature treatments ($p < 0.05$).

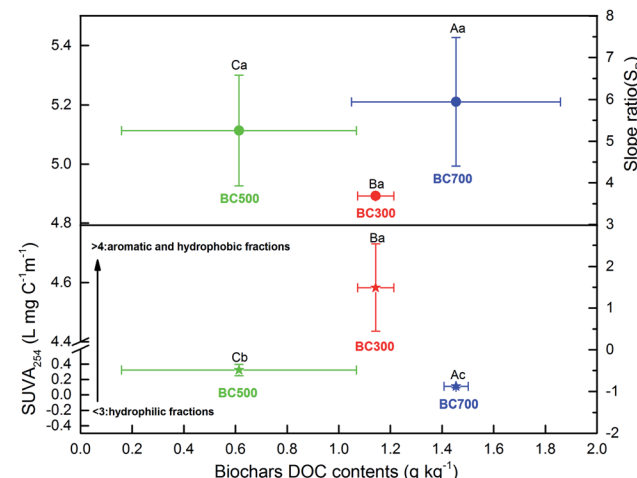


Fig. 4 The relationship between dissolved organic carbon (DOC) and specific UV absorbance at the wavelength (SUVA₂₅₄) or slope ratio (S_{254}) from UV absorbance of DOM derived from the biochar produced at different pyrolysis temperatures (300, 500 and 700 °C). All values are given as the mean \pm SD from three replicates. Different letters indicate statistical differences between different pyrolysis temperature treatments ($p < 0.05$).



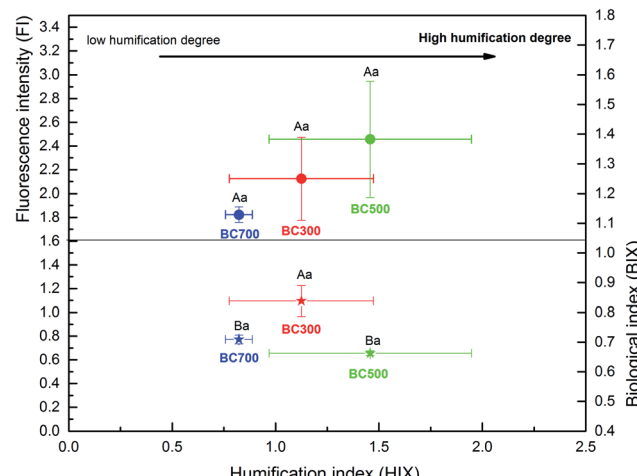


Fig. 5 Correlations of the humification index (HIX) with the biological index (BIX) and fluorescence index (FI) of DOM derived from the biochar produced at different pyrolysis temperatures (300, 500 and 700 °C). All values are given as the mean \pm SD from three replicates. Different letters indicate statistical differences between different pyrolysis temperature treatments ($p < 0.05$).

additional analyses of $SUVA_{254}$ and S_R were done by UV-visible spectrophotometry, and the correlation between DOC and the indices was also analysed (Fig. 4 and 5). The mean $SUVA_{254}$ of DOM released from biochar at 500 °C and 700 °C was 0.32 L mg

$C^{-1} m^{-1}$ and 0.11 L mg $C^{-1} m^{-1}$, respectively, which predicts a lower aromaticity of DOM ($SUVA_{254} < 1$) and more hydrophilic fractions ($SUVA_{254} < 3$).^{20,23,43} However, the $SUVA_{254}$ of DOM released from biochar produced at a low temperature (300 °C) was 4.58 L mg $C^{-1} m^{-1}$ higher than that released from biochar produced at a high temperature, which was significant ($p < 0.01$), indicating strong aromatic and abundant hydrophobic fractions.⁴⁴ Additionally, a significant change in S_R was found with the DOC content of biochar, and the high DOC concentration showed high S_R values, which were 3.69 (300 °C), 5.25 (500 °C) and 5.95 (700 °C). As the proxy of DOM molecular weight, the S_R value in this study was much higher at high pyrolysis temperatures, suggesting a large molecular weight with the increase in DOC concentration.⁴⁵ The relationship among the DOC concentration, $SUVA_{254}$, and S_R obtained in Fig. 4 revealed that the characteristics of DOM released from biochar could be regulated by the DOC content due to the various pyrolysis temperatures, which was consistent with previous results of Li *et al.*¹⁹

The indices of FI, BIX, and HIX are currently used to quantify the compositional variation and source of DOM. As shown in Fig. 5, the correlation between FI, BIX and HIX also displayed a significant difference with the biochar produced at different pyrolysis temperatures. The HIX values showed a negative relationship with the BIX index, while they showed a positive relationship to the FI index with the increase in the humification degree of biochar obtained at different pyrolysis

Table 2 Variations of UV-visible and fluorescent indices ($SUVA_{254}$, $SUVA_{260}$, FI, HIX, BIX, freshness) for soil profile (0–40 cm) after 55 days column leaching^a

Soil depth	Treatments	$SUVA_{254}$	$SUVA_{260}$	FI	HIX	BIX	$\beta : \alpha$
0–10 cm	CK	0.69 \pm 0.05bc	0.66 \pm 0.05bc	1.02 \pm 0.10b	0.52 \pm 0.10a	0.75 \pm 0.20a	0.65 \pm 0.16a
	CF	2.57 \pm 0.13a	2.45 \pm 0.13b	1.98 \pm 0.15a	0.98 \pm 0.15a	0.66 \pm 0.16a	0.60 \pm 0.14a
	RF	2.26 \pm 2.43ab	8.87 \pm 2.35a	1.83 \pm 0.10a	0.80 \pm 0.10a	0.56 \pm 0.01a	0.53 \pm 0.03a
	RFBC300	2.00 \pm 0.71bc	1.93 \pm 0.68bc	1.85 \pm 0.12a	0.75 \pm 0.12a	0.67 \pm 0.10a	0.61 \pm 0.09a
	RFBC500	0.49 \pm 0.13c	0.47 \pm 0.13c	2.00 \pm 0.09a	1.00 \pm 0.09a	0.56 \pm 0.20a	0.51 \pm 0.19a
	RFBC700	1.41 \pm 0.21bc	1.34 \pm 0.19b	1.20 \pm 0.21a	0.92 \pm 0.21a	0.73 \pm 0.21a	0.67 \pm 0.17a
10–20 cm	CK	6.15 \pm 1.65b	5.90 \pm 1.58b	1.87 \pm 0.12 ab	0.90 \pm 0.12a	0.61 \pm 0.03a	0.56 \pm 0.03a
	CF	1.53 \pm 0.39c	1.48 \pm 0.39c	1.84 \pm 0.12b	0.84 \pm 0.12b	0.59 \pm 0.05a	0.53 \pm 0.07a
	RF	0.78 \pm 0.12c	0.74 \pm 0.11c	1.83 \pm 0.08b	0.83 \pm 0.08b	0.71 \pm 0.06a	0.64 \pm 0.06a
	RFBC300	2.00 \pm 0.08c	1.91 \pm 0.08c	2.12 \pm 0.27a	1.12 \pm 0.26a	0.67 \pm 0.16a	0.57 \pm 0.16a
	RFBC500	9.86 \pm 1.77a	9.50 \pm 1.73a	1.85 \pm 0.12b	0.85 \pm 0.12b	0.29 \pm 0.21	0.26 \pm 0.19b
	RFBC700	1.48 \pm 1.08c	1.45 \pm 1.05c	1.74 \pm 0.05b	0.74 \pm 0.05b	0.58 \pm 0.03a	0.54 \pm 0.03a
20–30 cm	CK	2.59 \pm 0.31a	2.49 \pm 0.31a	1.79 \pm 0.06b	1.81 \pm 0.08b	0.59 \pm 0.05a	0.54 \pm 0.03a
	CF	3.64 \pm 1.39a	3.50 \pm 1.37a	2.14 \pm 0.23a	1.18 \pm 0.14a	0.64 \pm 0.12a	0.55 \pm 0.18a
	RF	4.33 \pm 1.58a	4.16 \pm 1.52a	1.83 \pm 0.17b	0.82 \pm 0.07b	0.52 \pm 0.15a	0.47 \pm 0.14a
	RFBC300	0.69 \pm 0.34b	0.68 \pm 0.33b	1.68 \pm 0.09b	0.66 \pm 0.07b	0.45 \pm 0.15a	0.43 \pm 0.16a
	RFBC500	3.00 \pm 0.48a	2.87 \pm 0.46a	1.76 \pm 0.12b	0.76 \pm 0.12b	0.59 \pm 0.10a	0.56 \pm 0.09a
	RFBC700	3.98 \pm 1.09a	3.79 \pm 1.04a	2.19 \pm 0.15a	1.19 \pm 0.15a	0.67 \pm 0.08a	0.59 \pm 0.11a
30–40 cm	CK	6.87 \pm 4.76ab	6.59 \pm 4.56ab	2.00 \pm 0.21ab	0.97 \pm 0.17c	0.67 \pm 0.11ab	0.63 \pm 0.09ab
	CF	0.46 \pm 0.11d	0.44 \pm 0.11d	1.62 \pm 0.11b	1.59 \pm 0.09b	0.34 \pm 0.02c	0.33 \pm 0.02c
	RF	3.39 \pm 0.99bcd	3.24 \pm 0.95 cd	1.76 \pm 0.06b	1.80 \pm 0.04b	0.55 \pm 0.03bc	0.52 \pm 0.02abc
	RFBC300	4.68 \pm 0.67abc	4.46 \pm 0.63bc	1.86 \pm 0.12ab	1.78 \pm 0.09ab	0.68 \pm 0.02ab	0.63 \pm 0.01ab
	RFBC500	7.84 \pm 1.79a	7.51 \pm 1.73a	2.32 \pm 0.57a	2.08 \pm 0.18a	0.52 \pm 0.25c	0.44 \pm 0.27bc
	RFBC700	0.75 \pm 0.19cd	0.73 \pm 0.20cd	1.93 \pm 0.17ab	0.89 \pm 0.12ab	0.84 \pm 0.08a	0.75 \pm 0.11a

^a $SUVA_{254}$: specific UV absorbance at wavelength 254 nm; $SUVA_{260}$: specific UV absorbance at wavelength 260 nm; FI: fluorescent index; HIX: humification index; BIX: biological index; $\beta : \alpha$: freshness index. Different letters indicate statistical differences between different treatments ($p < 0.05$).



temperatures (Fig. 5). The ranges of FI and HIX were 1.82–2.46 and 0.82–1.46, respectively, which indicate a microbial or autochthonous source (terrestrial and allochthonous: $1.2 < FI < 1.5$; microbial or autochthonous: $1.7 < FI < 2.0$) of DOM released from biochar produced at different pyrolysis temperatures.²⁹

Furthermore, the variations of UV-visible and fluorescent indices (SUVA₂₅₄, SUVA₂₆₀, FI, HIX, BIX, and freshness) of biochar-amended soil (0–40 cm) after 55 days of column leaching were also analysed (Table 2). Biochar amendments significantly increased the SUVA₂₅₄ and SUVA₂₆₀ values in topsoil (0–10 cm), which indicating strong aromatic and hydrophobic properties of soil DOM.^{9,19} Compared to CK treatment, obvious increase of FI and HIX indices were observed, which may attributed to the presence of fertilizer and biochar containing substituents, hydroxyl, alkoxy, amino groups, tending to shift fluorescence maxima to longer wavelengths.⁴⁶ However, for BIX and $\beta : \alpha$, there were no significant difference among the control and biochar amended treatments. With the increasing of depth, the SUVA₂₅₄ and SUVA₂₆₀ values showed a tendency of increasing, which may be attributed to the down transport of DOM with the process of leaching. However, the further study on the variations of soil and leachate DOM molecular weights in the process of leaching should be conducted to reveal the mechanisms of DOM migration and transformation. The distinct changes of present indices predicted a potential variation of soil DOM composition after biochar amendment and fertilizer addition during a period of leaching.

4. Conclusion

The DOM content derived from wheat straw biochar produced at different pyrolysis temperatures (300 °C, 500 °C and 700 °C) significantly varied, with a range of 0.61–1.45 g kg^{−1}, while the DOM minimum achieved at 500 °C. Moreover, the quantity and chemical quality of DOM derived from the biochar were analysed in using fluorescence and UV absorption techniques coupled with EEM-PARAFAC, and three fluorescent components (protein and tryptophan-like, UVA humic acid-like and UVC humic acid-like substances) were identified. Furthermore, the distributions of the three components suggested that more aromatic humic materials with higher molecular weights but poor amino acids were generated with the increase in pyrolysis temperature. The potential application of biochar in paddy soil was also evaluated by optical indices, and the findings demonstrated that biochar amendments could hasten soil DOM decomposition and transportation, resulting in the development of a soil/water environment or rice yield and quality.

Conflicts of interest

The authors confirm that there has no conflict of interest in this article.

Acknowledgements

This research was funded by the Shaanxi Science and Technology Coordination Innovation Project (2016KTZDNY03-01)

and the Shaanxi Water Resources Science and Technology Project (2016slkj-15).

References

- 1 M. H. Duku, S. Gu and E. B. Hagan, Biochar production potential in Ghana—a review, *Renewable Sustainable Energy Rev.*, 2011, **15**, 3539–3551.
- 2 D. Mohan, A. Sarswat, Y. S. Ok and C. U. Pittman Jr, Organic and inorganic contaminants removal from water with biochar, a renewable, low cost and sustainable adsorbent—a critical review, *Bioresour. Technol.*, 2014, **160**, 191–202.
- 3 J. Lehmann, J. Gaunt and M. Rondon, Biochar sequestration in terrestrial ecosystems – a review, *Mitig. Adapt. Strategies Glob. Change*, 2006, **11**(2), 403–427.
- 4 X. Liu, J. Zheng, D. Zhang, K. Cheng, H. Zhou, A. Zhang, L. Li, S. Joseph, P. Smith, D. Crowley, Y. Kuzyakov and G. Pan, Biochar has no effect on soil respiration across Chinese agricultural soils, *Sci. Total Environ.*, 2016, **554–555**, 259–265.
- 5 A. Zhang, X. Zhou, M. Li and H. Wu, Impacts of biochar addition on soil dissolved organic matter characteristics in a wheat-maize rotation system in loess plateau of China, *Chemosphere*, 2017, **186**(1), 986.
- 6 G. Agegnehu, A. M. Bass, P. N. Nelson and M. I. Bird, Benefits of biochar, compost and biochar-compost for soil quality, maize yield and greenhouse gas emissions in a tropical agricultural soil, *Sci. Total Environ.*, 2016, **543**, 295–306.
- 7 A. Zhang, L. Cui, G. Pan, L. Li, Q. Hussain and X. Zhang, Effect of biochar amendment on yield and methane and nitrous oxide emissions from a rice paddy from Tai Lake plain, China, *Agric. Ecosyst. Environ.*, 2010, **139**(4), 469–475.
- 8 Y. Feng, Y. Xu, Y. Yu, Z. Xie and X. Lin, Mechanisms of biochar decreasing methane emission from Chinese paddy soils, *Soil Biol. Biochem.*, 2012, **46**(1), 80–88.
- 9 J. Gao, J. Lv, H. Wu, Y. Dai and M. Nasir, Impacts of wheat straw addition on dissolved organic matter characteristics in cadmium-contaminated soils: insights from fluorescence spectroscopy and environmental implications, *Chemosphere*, 2017, **193**, 1027.
- 10 D. Wei, M. Li, X. Wang and F. Han, Extracellular polymeric substances for Zn (II) binding during its sorption process onto aerobic granular sludge, *J. Hazard. Mater.*, 2016, **301**, 407–415.
- 11 J. Tang, X. Li, Y. Luo, G. Li and S. Khan, Spectroscopic characterization of dissolved organic matter derived from different biochars and their polycyclic aromatic hydrocarbons (PAHs) binding affinity, *Chemosphere*, 2016, **152**, 399–406.
- 12 Y. F. Guan, B. C. Huang, C. Qian and H. Q. Yu, Quantification of Humic Substances in Natural Water Using Nitrogen-Doped Carbon Dots, *Environ. Sci. Technol.*, 2017, **51**, 14092–14099.
- 13 M. Uchimiya, T. Ohno and Z. Q. He, Pyrolysis temperature-dependent release of dissolved organic carbon from plant, manure, and biorefinery wastes, *J. Anal. Appl. Pyrolysis*, 2013, **104**(104), 84–94.



14 G. Li, S. Khan, M. Ibrahim, T. R. Sun, J. F. Tang, J. B. Cotner and Y. Y. Xu, Biochars induced modification of dissolved organic matter (DOM) in soil and its impact on mobility and bioaccumulation of arsenic and cadmium, *J. Hazard. Mater.*, 2018, **348**, 100–108.

15 P. Devi and A. K. Saroha, Effect of pyrolysis temperature on polycyclic aromatic hydrocarbons toxicity and sorption behaviour of biochars prepared by pyrolysis of paper mill effluent treatment plant sludge, *Bioresour. Technol.*, 2015, **192**, 312–320.

16 P. G. Coble, Characterization of marine and terrestrial DOM in seawater using excitation–emission matrix spectroscopy, *Mar. Chem.*, 1996, **51**, 325–346.

17 C. Guéguen, D. C. Burns, A. McDonald and B. Ring, Structural and optical characterization of dissolved organic matter from the lower Athabasca River, Canada, *Chemosphere*, 2012, **87**, 932–937.

18 C. A. Stedmon and R. Bro, Characterizing dissolved organic matter fluorescence with parallel factor analysis: a tutorial, *Limnol. Oceanogr. Methods*, 2008, **6**, 572–579.

19 M. Li, A. Zhang, H. Wu, H. Liu and J. Lv, Predicting potential release of dissolved organic matter from biochars derived from agricultural residues using fluorescence and ultraviolet absorbance, *J. Hazard. Mater.*, 2017, **334**, 86–92.

20 D. Wei, H. H. Ngo, W. Guo, W. Xu, B. Du and M. S. Khan, Biosorption performance evaluation of heavy metal onto aerobic granular sludge-derived biochar in the presence of effluent organic matter *via* batch and fluorescence approaches, *Bioresour. Technol.*, 2018, 410–416.

21 L. Huang, M. Li, H. H. Ngo, W. Guo, W. Xu and B. Du, Spectroscopic characteristics of dissolved organic matter from aquaculture wastewater and its interaction mechanism to chlorinated phenol compound, *J. Mol. Liq.*, 2018, **263**, 422–427.

22 S. K. L. Ishii and T. H. Boyer, Behavior of reoccurring PARAFAC components in fluorescent dissolved organic matter in natural and engineered systems: a critical review, *Environ. Sci. Technol.*, 2012, **46**, 2006–2017.

23 N. P. Sanchez, A. T. Skeriotis and C. M. Miller, Assessment of dissolved organic matter fluorescence PARAFAC components before and after coagulation-filtration in a full scale water treatment plant, *Water Res.*, 2013, **47**, 1679–1690.

24 M. Uchimiya, Z. Liu and K. Sistani, Field-scale fluorescence fingerprinting of biochar-borne dissolved organic carbon, *J. Environ. Manage.*, 2016, **169**, 184–190.

25 J. Sun, F. He and Y. Pan, Effects of pyrolysis temperature and residence time on physicochemical properties of different biochar types, *Acta Agric. Scand., Sect. B*, 2016, **67**(1), 1–11.

26 J. Paz-Ferreiro, S. Fu, A. Méndez and G. Gascó, Interactive effects of biochar and the earthworm *pontoscolex corethrurus*, on plant productivity and soil enzyme activities, *J. Soils Sediments*, 2014, **14**(3), 483–494.

27 J. Hur, S. J. Hwang and J. K. Shin, Using synchronous fluorescence technique as a water quality monitoring tool for an urban river, *Water, Air, Soil Pollut.*, 2008, **191**, 231–243.

28 Á. Zsolnay, The prediction of the environmental function of the dissolved organic matter in ecosystems, *Final Report of the Eur. Sci., Foundation Exploratory Workshop*, 2001.

29 D. M. McKnight, E. W. Boyer, P. K. Westerhoff, P. T. Doran, T. Kulbe and D. T. Andersen, Spectrofluorometric characterisation of dissolved organic matter for indication of precursor organic material and aromaticity, *Limnol. Oceanogr.*, 2001, **46**(1), 38–48.

30 H. F. Wilson and M. A. Xenopoulos, Effects of agricultural land use on the composition of fluvial dissolved organic matter, *Nat. Geosci.*, 2009, **2**, 37–41.

31 B. Marschner and K. Kalbitz, Controls of bioavailability and biodegradability of dissolved organic matter in soils, *Geoderma*, 2003, **113**(3e4), 211e235.

32 Y. Lin, P. Munroe, S. Joseph, R. Henderson and A. Ziolkowski, Water extractable organic carbon in untreated and chemical treated biochars, *Chemosphere*, 2012, **87**, 151–157.

33 A. Mukherjee and A. R. Zimmerman, Organic carbon and nutrient release from a range of laboratory-produced biochars and biochar-soil mixtures, *Geoderma*, 2013, **193–194**, 122–130.

34 D. A. Wardle, M. C. Nilsson and O. Zackrisson, Fire-derived charcoal causes loss of forest humus, *Science*, 2008, **320**, 629.

35 A. M. McIntyre and C. Guéguen, Binding interactions of algal-derived dissolved organic matter with metal ions, *Chemosphere*, 2013, **90**, 620–626.

36 W. Chen, P. Westerhoff, J. A. Leenheer and K. Booksh, Fluorescence excitation–emission matrix regional integration to quantify spectra for dissolved organic matter, *Environ. Sci. Technol.*, 2003, **37**, 5701–5710.

37 J. B. Fellman, E. Hood and R. G. Spencer, Fluorescence spectroscopy opens new windows into dissolved organic matter dynamics in freshwater ecosystems: A review, *Limnol. Oceanogr.*, 2010, **55**, 2452–2462.

38 C. Santín, Y. Yamashita, X. L. Otero, M. Á. Álvarez and R. Jaffé, Characterizing humic substances from estuarine soils and sediments by excitation–emission matrix spectroscopy and parallel factor analysis, *Biogeochemistry*, 2009, **96**(1), 131–147.

39 P. G. Coble, S. A. Green, N. V. Blough and R. B. Gagosian, Characterization of dissolved organic matter in the Black Sea by fluorescence spectroscopy, *Nature*, 1990, **348**(6300), 432–435.

40 D. Wei, K. Zhang, S. Wang, B. Sun, N. Wu and W. Xu, Characterization of dissolved organic matter released from activated sludge and aerobic granular sludge biosorption processes for heavy metal treatment *via* a fluorescence approach, *Int. Biodeterior. Biodegrad.*, 2017, **124**, 326–333.

41 A. Smebye, V. Alling, R. D. Vogt, T. C. Gadmar, J. Mulder, G. Cornelissen and S. E. Hale, Biochar amendment to soil changes dissolved organic matter content and composition, *Chemosphere*, 2016, **142**, 100–105.

42 M. Uchimiya, I. M. Lima, K. Thomas Klasson, S. Chang, L. H. Wartelle and J. E. Rodgers, Immobilization of heavy metal ions (CuII, CdII, NiII, and PbII) by broiler litter-



derived biochars in water and soil, *J. Agric. Food Chem.*, 2010, **58**, 5538–5544.

43 Y. L. Yeh, K. J. Yeh, L. F. Hsu, W. C. Yu, M. H. Lee and T. C. Chen, Use of fluorescence quenching method to measure sorption constants of phenolic xenoestrogens onto humic fractions from sediment, *J. Hazard. Mater.*, 2014, **277**, 27–33.

44 A. Matilainen, E. T. Gjessing, T. Lahtinen, L. Hed, A. Bhatnagar and M. Sillanpää, An overview of the methods used in the characterisation of natural organic matter (nom) in relation to drinking water treatment, *Chemosphere*, 2012, **83**(11), 1431e1442.

45 Y. Yamashita, N. Maie, H. Briceno and R. Jaffe, Optical characterization of dissolved organic matter in tropical rivers of the Guayana Shield, Venezuela, *J. Geophys. Res.*, 2010, **115**, 214–221.

46 F. J. Rodríguez, P. Schlenger and M. García-Valverde, A comprehensive structural evaluation of humic substances using several fluorescence techniques before and after ozonation. Part I: structural characterization of humic substances, *Sci. Total Environ.*, 2014, **476**(3), 718e730.

47 C. A. Stedmon and S. Markager, Resolving the variability in dissolved organic matter fluorescence in a temperate estuary and its catchment using PARAFAC analysis, *Limnol. Oceanogr.*, 2005, **50**(2), 686e697.

48 T. Jamieson, E. Sager and C. Guéguen, Characterization of biochar-derived dissolved organic matter using UV-visible absorption and excitation-emission fluorescence spectroscopies, *Chemosphere*, 2014, **103**(5), 197–204.

